Journal of Catalysis **191,** 438–444 (2000)
doi:10.1006/jcat.1999.2808, available online at http://www.idealibrary.com on IDEAL®

Formation, Structure, and HDN Activity of Unsupported Molybdenum Phosphide

C. Stinner, R. Prins, and Th. Weber[1]

Laboratory for Technical Chemistry, Swiss Federal Institute of Technology (ETH), 8092 Zurich, Switzerland

Received October 1, 1999; revised December 14, 1999; accepted December 15, 1999

A molybdenum phosphide catalyst was prepared from an aqueous solution of $(NH_4)_6Mo_7O_{24}\cdot 4H_2O$ and $(NH_4)_2HPO_4$ by precipitation, calcination, and subsequent reduction in H_2 at 923 K. Raman spectroscopic measurements revealed that the aqueous solution contained MoO_4^{2-}, HPO_4^{2-}, and $P_2Mo_5O_{23}^{6-}$ anions. Powder XRD measurements showed that pure molybdenum phosphide had formed after precipitation and reduction with H_2. MoP crystallizes in the tungsten carbide structure in which each Mo atom is trigonal-prismatically coordinated by six P atoms. The molybdenum phosphide was tested for catalytic activity in the HDN reaction of *o*-propylaniline at 643 K and 3.0 MPa. The intrinsic HDN activity of the surface Mo atoms of MoP was about 6 times higher than that of Mo edge atoms in γ-Al_2O_3-supported MoS_2. Their selectivity is comparable to that of an Ni-promoted MoS_2 catalyst.

Key Words: **molybdenum; phosphides; catalyst preparation; molybdophosphates; Raman spectroscopy; hydrodenitrogenation.**

1. INTRODUCTION

Transition metal sulfides are widely used as catalysts in the field of hydrodesulfurization (HDS) and hydrodenitrogenation (HDN) (1–3). The removal of sulfur- and nitrogen-containing compounds from fuels is essential for SO_2 and NO_x abatement. In view of more stringent environmental legislation, more efforts must be made to lower the levels of sulfur and nitrogen in fuels. To meet these future demands either existing catalysts have to be improved, for which a detailed understanding of structure and catalytic action is required, or alternative catalysts have to be found. Besides the sulfides of transition metals, carbides and nitrides have been tested and proved to be catalytically active as well (4–7). In comparison with sulfidic HDN catalysts, molybdenum nitrides behave more like metals, resulting in a higher selectivity to hydrogenolysis products (5).

In contrast to the extent of research focused on nitrides and carbides, transition metal phosphides have been less explored (8, 9). Phosphides or mixed phosphide sulfides have been considered as HDN or HDS catalysts in only a few cases, such as Ni_2P in the HDN of quinoline (10) and $NiPS_3$ in the HDS of thiophene (11). Recently molybdenum phosphide, MoP, has been prepared by a new method and tested for catalytic activity in the HDN of quinoline (12). In all these cases phosphides proved to be catalytically active.

Phosphorus in the form of phosphate is also used as a promoter in commercial hydrotreating catalysts which contain sulfided Ni (or Co) and Mo on an alumina support (13, 14). In the past two decades, phosphorus has been especially incorporated in $NiMo/Al_2O_3$ HDN catalysts (15) because industrial performance as well as studies with model compounds demonstrated a substantial promotional effect of phosphorus in such catalysts in HDN (15–18), whereas only a weak promotional effect in HDS was observed (16, 18, 19).

Phosphorus is introduced during catalyst preparation in the impregnation solution in the form of phosphate, and in this form it reacts with molybdate to give phosphomolybdate, thus enhancing the Mo solubility and stability in solution (20). Apart from this industrially very important physical effect, phosphate also influences the catalysis. Many studies have been done in an attempt to explain the catalytic function of phosphorus in $NiMoP/Al_2O_3$ HDN catalysts (16, 18, 21). Jian and Prins showed that the effect of phosphate depends on the reaction type (22). Phosphate strongly increases the rates of hydrogenation reactions such as the hydrogenation of aniline, benzene, and cyclohexene. How phosphate can improve the hydrogenation capacity of an $NiMo/Al_2O_3$ catalyst is not immediately clear. A kinetic study showed that phosphate increases the rate constant of the hydrogenation of *o*-propylaniline as well as its adsorption constant (23). This indicates that phosphate changes the nature of the sites.

One idea, already suggested some years ago (10, 24), is that phosphate may react with Ni–MoS_2 to form a catalyst with (partly) phosphide-like character. To test this idea, we have prepared pure MoP by a method published recently (12), and tested it in the HDN of *o*-propylaniline. *o*-Propylaniline is a simple test molecule but nevertheless it

[1] To whom correspondence should be addressed. Fax: +41 1 632 1162. E-mail: thomas.weber@tech.chem.ethz.ch.

0021-9517/00 $35.00

allows us to study several reactions involved in the HDN of N-containing aromatic compounds (hydrogenation of the phenyl ring, hydrogenolysis of the C(sp^2)–N bond, elimination of NH_3 from cyclohexylamine, and hydrogenation of cyclohexene), and all of these reactions have been well studied (23). Our aim was to test the capability of MoP compared to those of classical MoS_2 catalysts. To make a reasonable comparison between two different catalysts possible, we estimated for both catalysts the number of active centers at the surface.

2. EXPERIMENTAL

Preparation and Characterization of the Catalysts

Molybdenum phosphide was prepared as follows: 4.0 g of ammonium heptamolybdate $(NH_4)_6Mo_7O_{24}\cdot 4H_2O$ (3.24 mmol, Fluka, puriss. p.a.) and 3.0 g of diammonium hydrogen phosphate $(NH_4)_2HPO_4$ (22.72 mmol, Fluka, puriss. p.a.) were dissolved in deionized water to give a total volume of 15 ml of solution. After evaporation of water the obtained white solid was calcined in air at 773 K for 5 h and subsequently reduced in a stream of H_2 (99.999%, 150 ml $\cdot$ min^{-1}) at 923 K (heating rate 1 K $\cdot$ min^{-1}). During this sequence the color of the sample changes from white via dark blue (calcination) to black (reduction). Finally, the surface of the samples was passivated in a flow of 0.5% O_2/He (30 ml $\cdot$ min^{-1}) for 2 h at room temperature. The passivated MoP can be handled in air.

An Mo/γ-Al_2O_3 catalyst in the oxidic form with 8% Mo loading was prepared by pore volume impregnation of γ-Al_2O_3 extrudates (Condea, 210 m^2/g, pore volume 0.45 ml/g) with a solution prepared from $(NH_4)_6Mo_7O_{24}\cdot 4H_2O$. The impregnated sample was dried at 393 K for 9 h and then calcined in air at 773 K (5 h, heating rate 2 K/min). The calcined sample was crushed and sieved, after which the 63–125-μm fraction was used for the catalytic testing.

Fourier transform Raman measurements were carried out with a Raman module FRA 106/S equipped with a liquid nitrogen cooled Ge detector, a Nd:YAG laser (1064 nm, 500 mW), and a CaF_2 beamsplitter. The instrument was attached to a Bruker EQUINOX 55 spectrometer; data collection and processing were controlled by the OPUS 2.2 software (Bruker). Spectra were recorded at 2 cm^{-1} resolution, and the number of accumulated scans for each sample was 1024 scans. Solids were measured in aluminum sample cups and solutions in glass tubes in the 180° scattering geometry. Since the pH of an aqueous solution of $(NH_4)_6Mo_7O_{24}\cdot 4H_2O$ and $(NH_4)_2HPO_4$, prepared as described above, is 8.5, molybdate and phosphate reference solutions were adjusted to this value by addition of ammonia.

Thermogravimetric analyses were performed on a Mettler Toledo TGA/SDTA851^e instrument in flowing air at a heating rate of 10 K/min to 973 K. STAR^e 5.1 software (Mettler Toledo) was used for data evaluation. XRD measurements were done with a STOE STADI P powder diffractometer (Cu $K\alpha_1$ radiation, Ge monochromator, PSD detector). For the measurements, the sample was filled into a 0.1-mm capillary. Nitrogen adsorption isotherms were measured at 77 K with a Micromeritics ASAP 2000M instrument. The surface area was determined by the BET method.

HDN Activity Measurements

The catalytic tests for the HDN of *o*-propylaniline were carried out in a continuous-flow microreactor at a total pressure of 3.0 MPa. A sample of 0.3 g of MoP or 0.05 g of Mo/γ-Al_2O_3 catalyst diluted with 8 g of SiC was used for each reaction. To remove oxygen from the surface of the passivated MoP catalyst, the catalyst was activated *in situ* with H_2 at 673 K and 0.1 MPa for 3 h. In the case of the Mo/γ-Al_2O_3 catalyst the sample was activated by sulfidation in a 10% H_2S/H_2 flow (35 ml/min) at 673 K for 4 h. The liquid reactant was fed to the reactor by means of a high-pressure pump, with *n*-octane as the solvent. The catalyst was stabilized at 643 K and 3.0 MPa for 12 h before samples were taken. Variation of space time was achieved by changing the flow rate while keeping the ratio between liquid feed and H_2 gas flow constant. The product stream was analyzed online with a Varian 3800 gas chromatograph equipped with an FID detector. The initial reactant partial pressure of *o*-propylaniline was 3 kPa. The experiments were carried out either in the absence of H_2S or at a partial H_2S pressure of 3 kPa by addition of dimethyl disulfide to the feed. *n*-Heptane was used as internal standard. Further details can be found in Ref. (23).

3. RESULTS AND DISCUSSION

Preparation and Characterization

Raman spectra of the educts and of a reaction intermediate of MoP are shown in Fig. 1 and compiled in Table 1. The Raman spectrum of an aqueous solution of $(NH_4)_6Mo_7O_{24}\cdot 4H_2O$ (Fig. 1a) shows bands at 895, 840, and 315 cm^{-1}. These bands are due to the ν_s(Mo=O), ν_{as}(Mo=O), and $\delta(MoO_2)$ vibrations of the MoO_4^{2-} anion (25), respectively, which forms from $Mo_7O_{24}^{6-}$ at a pH value of 8.5 by several hydration and deprotonation steps (26). The Raman spectrum of an aqueous solution of $(NH_4)_2HPO_4$ is shown in Fig. 1b. The band with the highest intensity at 986 cm^{-1} is due to the ν_s(P=O) vibration of the HPO_4^{2-} anion and is the most characteristic vibrational feature of this anion (27). Our Raman spectrum clearly shows that the HPO_4^{2-} anion is the main component of the solution. Based on the pK_a values of phosphoric acid, H_3PO_4 (28), an aqueous solution of $(NH_4)_2HPO_4$ should contain the HPO_4^{2-} and $H_2PO_4^{2-}$ anions in a ratio of 0.86 : 0.13.

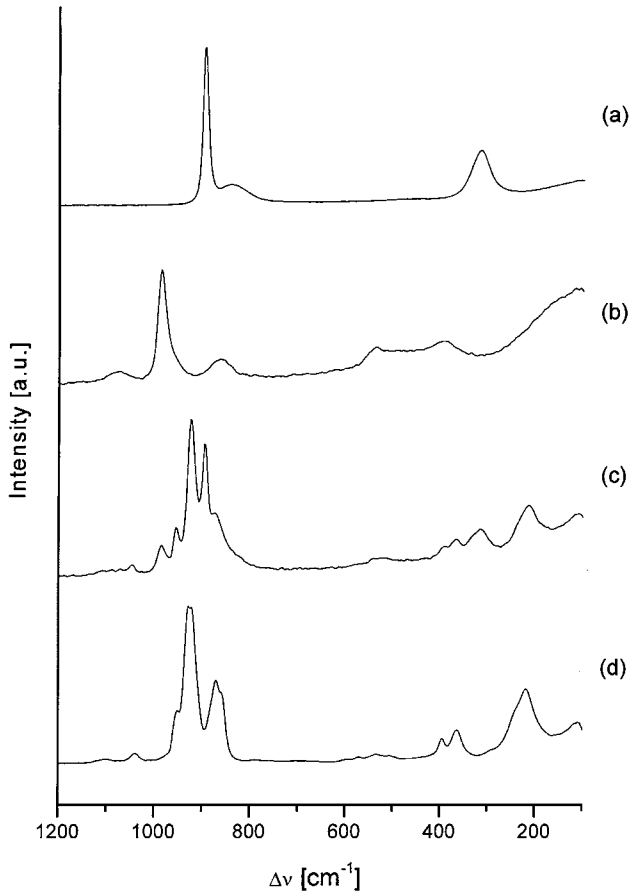

FIG. 1. FT Raman spectra of aqueous solutions of $(NH_4)_6Mo_7O_{24} \cdot 4H_2O$, $c(Mo) = 1.51\,mol \cdot l^{-1}$ (a); $(NH_4)_2HPO_4$, $c(P) = 1.51\,mol \cdot l^{-1}$ (b); and $(NH_4)_6Mo_7O_{24} \cdot 4H_2O$ and $(NH_4)_2HPO_4$, $c(Mo) = c(P) = 1.51\,mol \cdot l^{-1}$ (c). Raman spectrum of sample c after evaporation (d).

The more intense bands of spectra a and b are present in spectrum c as well, but in addition there are new bands at 1047, 955, 924, 531, and 213 cm^{-1} (Fig. 1c). These bands can be assigned to the phosphomolybdate $P_2Mo_5O_{23}^{6-}$ anion (29). The only difference between our spectrum and that reported by Lyhamn and Pettersson (29) is the position of the band with highest intensity, which we observe at 932 cm^{-1} rather than at 924 cm^{-1}. However, the general appearance is the same in both cases. From the results presented so far, we conclude that an aqueous solution of $(NH_4)_6Mo_7O_{24} \cdot 4H_2O$ and $(NH_4)_2HPO_4$ contains the MoO_4^{2-}, HPO_4^{2-}, and $P_2Mo_5O_{23}^{6-}$ anions as the main components.

Upon evaporation, a white solid is obtained. The Raman spectrum of this material is shown in Fig. 1d. The bands at 951 and 920 cm^{-1} can again be assigned to the $P_2Mo_5O_{23}^{6-}$ anion, where slight shifts in the positions of the bands must be taken into account when comparing solution with solid-state spectra. While bands related to the MoO_4^{2-} anion cannot be observed anymore, the new bands at 929 and 871 cm^{-1} are due to ν(Mo–O) stretching vibrations of the $Mo_7O_{24}^{6-}$ anion in the solid state. An unequivocal assignment of the bands at 364 and 219 cm^{-1} is difficult, because the $P_2Mo_5O_{23}^{6-}$ as well as the $Mo_7O_{24}^{6-}$ ion exhibit bands in this region. Vibrational features due to the presence of free phosphate are mostly obscured by the bands of heptamolybdate, because the Raman intensity of the latter is much higher than those of the phosphates. Since the structural chemistry of phosphates is very rich, i.e., polyphosphate chains and rings of different lengths can be formed by condensation processes, the presence of polyphosphates is likely. In this case additional bands due to ν(P–O) and $\delta(PO_2)$ vibrations of polyphosphates are expected in the spectral regions 850–1100, 500–550, and 350–400 cm^{-1}, as well as around 200 cm^{-1}.

Our TGA measurements are also in favor of the presence of polyphosphate species. For a mixture containing only $(NH_4)_6Mo_7O_{24}$ and $(NH_4)_2HPO_4$, the expected weight loss is 30.4%, according to

$$2(NH_4)_6Mo_7O_{24} \cdot 4H_2O + 14(NH_4)_2HPO_4$$
$$\rightarrow 14MoO_3 \cdot 7P_2O_5 + 40NH_3 + 35H_2O.$$

The weight loss in the case of our white solid, however, is 19%. This can only be explained by the condensation of $H_xPO_4^{(x-3)}$ anions ($x = 1$–3) to polyphosphate chains and rings during the evaporation process, accompanied by the loss of H_2O and NH_3.

Calcination of the white Mo–P–O precursor leads to the formation of a dark blue, amorphous compound. The dark blue color has also been observed in other molybdenum compounds, e.g., molybdenum phosphate glasses (30). This phenomenon may be explained by the formation of Mo^{5+} centers during calcination accompanied by the loss of oxygen. The blue color results from intervalence charge-transfer transitions between Mo^{5+} and Mo^{6+} centers (31).

Bridge and Patel (32) discussed in their studies on the vitreous Mo–P–O system a structural model for Mo–P–O glasses containing 50 mol% Mo. They proposed a structure of an interlinked network of proximate MoO_6 octahedra and PO_4 tetrahedra. The model shows a high occurrence of MoO_6 octahedra separated by only a single PO_4 group. The high homogeneity of Mo and P atoms in the amorphous oxidic precursor means low diffusion path lengths in the formation of the MoP structure, which may explain why the reduction to the MoP phase takes place at low temperatures.

Reduction of the blue compound in H_2 yields the black MoP material. The XRD pattern of the passivated MoP catalyst (Fig. 2) is in accordance with literature data reported for the crystalline solid-state compound MoP (33). Molybdenum phosphide crystallizes in the hexagonal tungsten carbide (WC) structure; each molybdenum atom is trigonal-prismatically surrounded by six phosphorus atoms, and vice versa (Fig. 3). In contrast to the layered structure of MoS_2, the three-dimensional structure of MoP allows a much better definition of the ratio of surface to bulk centers.

TABLE 1

Raman Bands and Assignments of the Spectra Shown in Fig. 1

$(NH_4)_6Mo_7O_{24}\cdot 4H_2O$[a]	$(NH_4)_2HPO_4$	$(NH_4)_6Mo_7O_{24}\cdot 4H_2O$/ $(NH_4)_2HPO_4$	White solid after evaporation	Assignment
	1072 (w[b])		1099 (br)	ν(P–O)
		1047 (w)	1039 (w)	
	986 (vs)	986 (m)		ν_s(P–O), HPO_4^{2-}
		955 (m)	951 (sh)	ν(Mo–O)/ν(P–O)
		924 (vs)	929 (vs)	
			920 (vs)	
895 (vs)		895 (s)		ν_s(Mo–O), MoO_4^{2-}
		874 (sh)	871 (s)	ν(Mo–O)/ν(P–O)
	863 (w)			ν_s(P–(OH))/ν_s(P–$(OH)_2$)
			856 (sh)	ν(Mo–O)/ν(P–O)
840 (w)				ν_{as}(Mo–O), MoO_4^{2-}
			595 (w/br)	$\delta(PO_2)$/
			572 (w/br)	$\delta(MoO_2)$
	536 (w)	531 (w/br)	533 (w)	
			505 (w/br)	
	395 (w)	392 (w)	395 (m)	
		367 (m)	364 (m)	
315 (m)		315 (m)		$\delta(MoO_2)$, MoO_4^{2-}
			244 (sh)	$\delta(PO_2)$/
			219 (s)	$\delta(MoO_2)$
		213 (s)	213 (sh)	

[a] $Mo_7O_{24}^{6-}$ decomposes in solution at pH 8.5 to MoO_4^{2-}.
[b] vs = very strong, s = strong, m = medium, w = weak, sh = shoulder, br = broad.

Activity Measurements

Prior to the determination of the catalyst activity, the MoP sample was reactivated in an H_2 flow at 673 K for 3 h. Activity measurements in the *o*-propylaniline HDN were performed in the absence and in the presence of H_2S. The results are displayed in Fig. 4. In the presence of H_2S the HDN activity is clearly lower. The influence of H_2S becomes

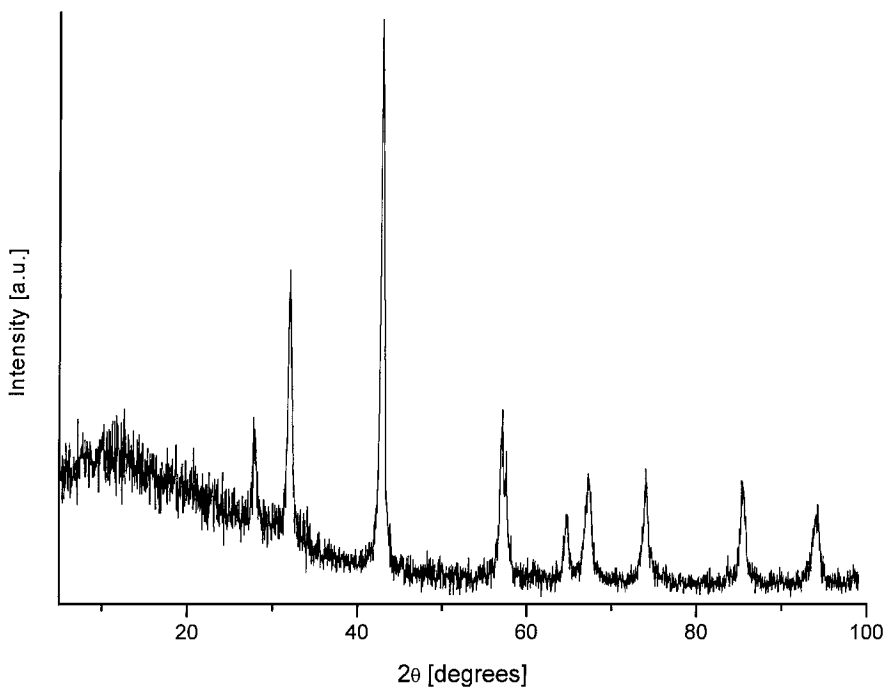

FIG. 2. Powder XRD pattern of the passivated MoP catalyst.

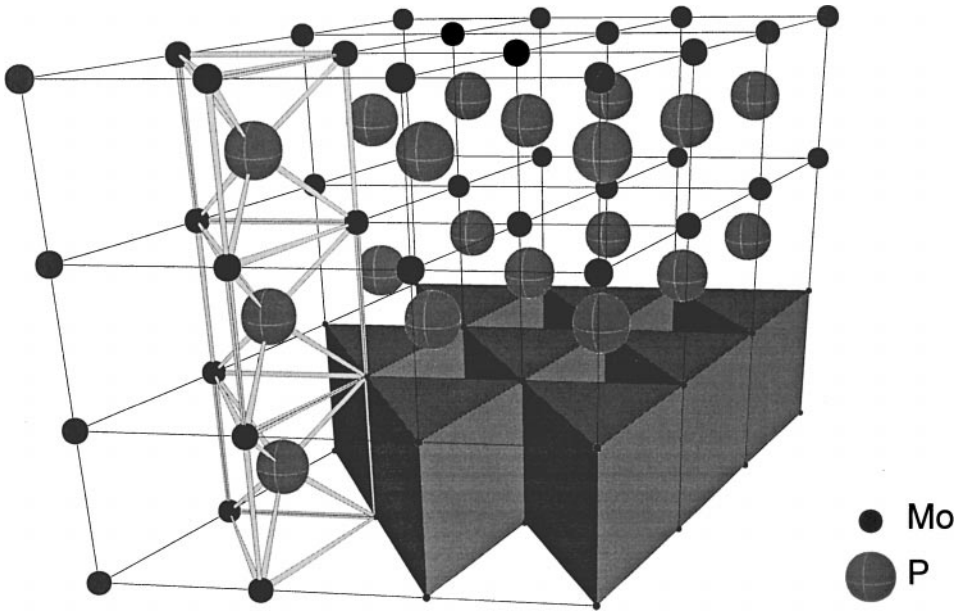

FIG. 3. Structure of molybdenum phosphide.

immediately effective, implying a fast blocking of surface catalytic sites. No deactivation was observed within 72 h.

The product selectivities are shown in Fig. 5. Propylcyclohexane, propylcyclohexenes, and propylbenzene are the main products, while hydrogenolysis products, such as ethylbenzene, toluene, and benzene, could not be detected. This property is different from that of the molybdenum nitrides. They behave more like metals, and hydrogenolysis products are formed in significant amounts during catalysis (5). The product distribution in the HDN reaction of *o*-propylaniline over the MoP catalyst resembles very much that over phosphate-promoted sulfidic $NiMo/Al_2O_3$ but is different from that over Mo/Al_2O_3 catalysts (23). Figure 6 shows the HDN reaction network for the reaction of *o*-propylaniline over the MoP catalyst. The same kind of network has been reported for $NiMo\{P\}/Al_2O_3$ catalysts (23, 34). The influence of H_2S is mainly a decrease in activity; the product distribution shows only minor changes.

Comparison between MoP and MoS_2 Catalysts

In order to estimate how the activity of MoP compares with that of MoS_2 in the HDN reaction we made a comparison of the activities for both catalyst types. We

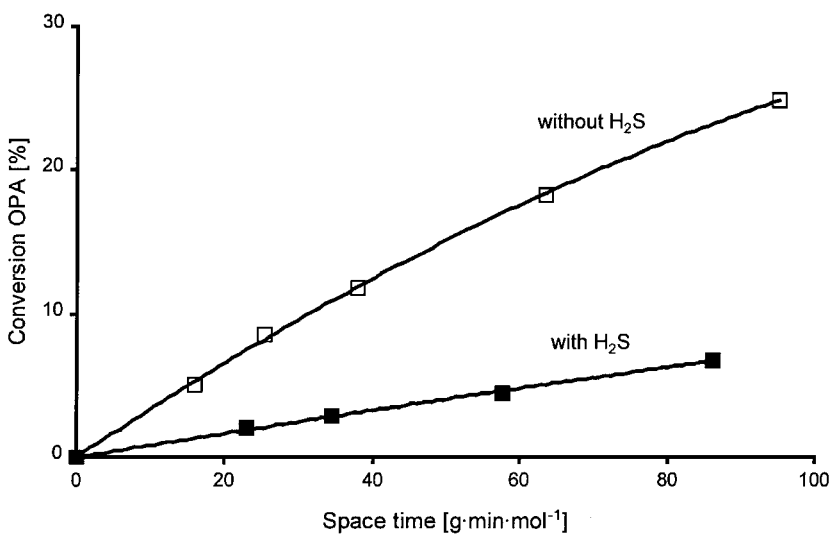

FIG. 4. HDN conversion of *o*-propylaniline over MoP in the presence and in the absence of H_2S.

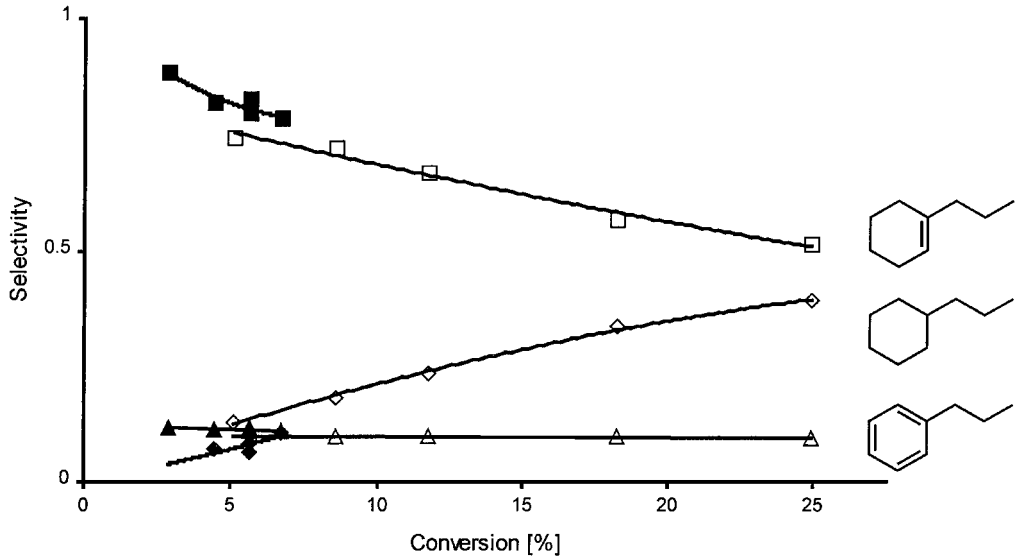

FIG. 5. Selectivities of products formed during the HDN of *o*-propylaniline over MoP in the absence (open symbols) and in the presence (closed symbols) of H_2S.

compared the supported MoS_2 catalyst with an unsupported MoP catalyst because preliminary experiments in which we tried to prepare supported MoP catalysts with the same method as that used for the unsupported MoP did not succeed. According to X-ray diffraction, Mo metal formed on the support under these conditions. However, although it might seem more straightforward to compare a supported catalyst with a supported model catalyst, this does not necessarily mean that this is the best way of estimating the intrinsic potential of MoP. When nothing is known about the geometry of MoP particles on a support, the comparison of the activities of these particles with those of MoS_2 particles on a support is meaningless.

Due to their different structures, MoP and MoS_2 cannot directly be compared. We based our comparison on an estimation of the number of active metal centers at the surface. One gram of our supported MoS_2 catalyst (8 wt% Mo on γ-Al_2O_3) contains 5.02×10^{20} Mo atoms. Assuming hexagonal MoS_2 platelets with a diameter of approximately 25 Å, as proposed by Shido and Prins on the basis of EXAFS measurements (35), one platelet contains 61 Mo atoms of

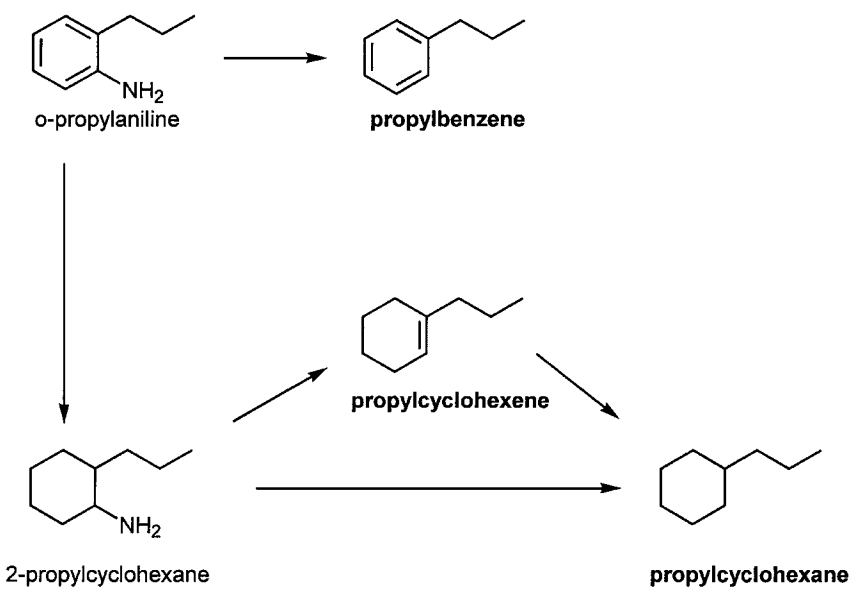

FIG. 6. HDN reaction network of *o*-propylaniline.

which 24 atoms are located at the edges. Thus, 1 g of catalyst contains 1.98×10^{20} Mo edge centers.

The number of surface Mo atoms in the unsupported MoP catalyst can be calculated if it is assumed that low index crystal planes, e.g., the (10$\bar{1}$0) or the (0001) crystal planes, constitute the surface of MoP. In that case each surface Mo atom occupies an area of 10.3 Å^2 (33). According to our BET measurements, the mesoporous surface area of the MoP catalyst is 2 m^2/g. Thus, 1 g of unsupported MoP would have 1.94×10^{19} Mo surface atoms, which is only 10% of the number of edge atoms in 1 g of the supported MoS_2 catalyst.

We assume that edge atoms in the case of the MoS_2/Al_2O_3 catalyst and surface atoms in the case of the MoP catalyst are the catalytically active centers in the HDN reaction. This allows us to make a direct comparison between the two catalyst types by calculating the turnover numbers. Under the same reaction conditions (643 K, 3.0 MPa, absence of H_2S, and flow rate of 5.26×10^{-8} mol/s) the *o*-propylaniline conversion is 6.9% for 0.05 g of MoS_2/Al_2O_3 and 24.9% for 0.3 g of MoP. Taking into account the amounts of catalyst used in the reaction and their number of Mo surface centers, this gives a turnover number of 2.2×10^{-4} molecules $\cdot$ (Mo center)$^{-1} \cdot$ s^{-1} for the MoS_2 catalyst and of 13.6×10^{-4} molecules $\cdot$ (Mo center)$^{-1} \cdot$ s^{-1} for the MoP catalyst. Thus, the MoP catalyst is intrinsically 6 times more active than the MoS_2/Al_2O_3 catalyst.

Even if these values should be treated with care, they unequivocally demonstrate that MoP has an intrinsically higher activity than MoS_2 for the HDN of *o*-propylaniline at 643 K and 3.0 MPa total pressure. This leaves the possibility open that small amounts of MoP on the surface of the sulfidic catalysts explain the phosphate effect in the HDN reaction over sulfidic NiMo{P}/Al_2O_3 catalysts. The addition of phosphate to HDN catalysts is known to have a strong promoting effect for HDN. After having demonstrated that MoP is intrinsically more active than MoS_2, we suggest that the MoP surface species might form from MoS_2 and phosphate under the reductive conditions of the HDN reaction.

Usually Ni is present as a promoter in supported MoS_2 HDN catalysts. Since the selectivity of MoP resembles that of an NiMoP/Al_2O_3 catalyst and not that of an MoS_2/Al_2O_3 catalyst, nickel phosphide may be formed instead of or in addition to MoP. The preparation of nickel phosphide and the determination of its catalytic activity in the HDN of *o*-propylaniline will, therefore, be the next step in our investigation of transition metal phosphide catalysts.

ACKNOWLEDGMENTS

We thank Mr. Fabio Rota for his help with the catalytic experiments.

REFERENCES

1. Prins, R., de Beer, V. H. J., and Somorjai, G. A., *Catal. Rev.-Sci. Eng.* **31**, 1 (1989).
2. Topsøe, H., Clausen, B. S., and Massoth, F. E., "Hydrotreating Catalysis." Springer, New York, 1996.
3. "Transition Metal Sulphides—Chemistry and Catalysis" (Th. Weber, R. Prins, and R. A. van Santen, Eds.). Kluwer, Dordrecht, 1998.
4. Schlatter, J. C., Oyama, S. T., Metcalfe, J. E., and Lambert, J. M., *Ind. Eng. Chem. Res.* **27**, 1648 (1988).
5. Abe, H., Cheung, T. K., and Bell, A. T., *Catal. Lett.* **21**, 11 (1993).
6. Aegerter, P. A., Quigley, W. W. C., Simpson, G. J., Ziegler, D. D., Logan, J. W., McCrea, K. R., Glazier, S., and Bussell, M. E., *J. Catal.* **164**, 109 (1996).
7. "The Chemistry of Transition Metal Carbides and Nitrides" (S. T. Oyama, Ed.). Blackie Academic and Professional, London, 1996.
8. Muetterties, E. L., and Sauer, J. C., *J. Am. Chem. Soc.* **96**, 3410 (1974).
9. Nozaki, F., and Tokumi, M., *J. Catal.* **79**, 207 (1983).
10. Robinson, W., van Gestel, J. N. M., Koranyi, T. I., Eijsbouts, S., van der Kraan, A. M., van Veen, J. A. R., and de Beer, V. H. J., *J. Catal.* **161**, 539 (1996).
11. Andreev, A., Vladov, C., Prahov, L., and Atanasova, P., *Appl. Catal. A-Gen.* **108**, L97 (1994).
12. Li, W., Dhandapani, B., and Oyama, S. T., *Chem. Lett.* 207 (1998).
13. Heresnape, J. N., and Morris, J. E., British Patent 701 217 (1953).
14. Housam, J. N., and Lester, R., British Patent 807 583 (1959).
15. van Veen, J. A. R., Colijn, H. A., Hendriks, P., and van Welsenes, A. J., *Fuel Process. Technol.* **35**, 137 (1993).
16. Fitz, C. W., and Rase, H. F., *Ind. Eng. Chem. Prod. Res. Dev.* **22**, 40 (1983).
17. Tischer, R. E., Narain, N. K., Stiegel, G. J., and Cillo, D. L., *Ind. Eng. Chem. Res.* **26**, 422 (1987).
18. Eijsbouts, S., van Gestel, J. N. M., van Veen, J. A. R., de Beer, V. H. J., and Prins, R., *J. Catal.* **131**, 412 (1991).
19. Bouwens, S., van der Kraan, A. M., de Beer, V. H. J., and Prins, R., *J. Catal.* **128**, 559 (1991).
20. Mickelson, G. A., U.S. Patents 3 749 633, 3 749 664, 3 755 148, 3 755 150, and 3 755 196 (1973).
21. Ramirez de Agudelo, M. M., and Morales, A., *in* "Proceedings, 9th Int. Congress on Catalysis, Calgary, 1988" (M. J. Philips and M. Ternan, Eds.), p. 42. Chem. Institute of Canada, Ottawa, 1988.
22. Jian, M., and Prins, R., *Catal. Lett.* **35**, 193 (1995).
23. Jian, M., Kapteijn, F., and Prins, R., *J. Catal.* **168**, 491 (1997).
24. Mangnus, P. J., van Langeveld, A. D., de Beer, V. H. J., and Moulijn, J. A., *Appl. Catal.* **68**, 161 (1991).
25. Nakamoto, K., "Infrared and Raman Spectra of Inorganic and Coordination Compounds." Wiley, New York, 1997.
26. Luthra, N. P., and Cheng, W. C., *J. Catal.* **107**, 154 (1987).
27. Niaura, G., Gaigalas, A. K., and Vilker, V. L., *J. Phys. Chem. B* **101**, 9250 (1997).
28. "Lange's Handbook of Chemistry" (J. A. Dean, Ed.). McGraw-Hill, New York, 1985.
29. Lyhamn, L., and Pettersson, L., *Chem. Scr.* **12**, 142 (1977).
30. Boudlich, D., Haddad, M., Nadiri, A., Berger, R., and Kliava, J., *J. Non-Cryst. Solids* **224**, 135 (1998).
31. Yamase, T., *Chem. Rev.* **98**, 307 (1998).
32. Bridge, B., and Patel, N. D., *J. Mater. Sci.* **21**, 1187 (1986).
33. Rundqvist, S., and Lundstrom, T., *Acta Chem. Scand.* **17**, 37 (1963).
34. Prins, R., *in* "Handbook of Heterogeneous Catalysis" (G. Ertl, H. Knözinger, and J. Weitkamp, Eds.), Vol. 4, p. 1908. VCH, Weinheim, 1997.
35. Shido, T., and Prins, R., *J. Phys. Chem. B* **102**, 8426 (1998).